Theoretical study of phosphate adsorption from wastewater using Al-(hydr)oxide

Nancy Y. Acelas*, Elizabeth Flórez

Departamento de Ciencias Básicas, Universidad de Medellín, Colombia, Carrera 87 No. 30-65, Medellín, Colombia, Tel. 57 4 3405278; email: nyacelas@udem.edu.co

ABSTRACT

The overabundance of phosphorus in water causes eutrophication of aquatic environments. As a consequence, developing an adsorbent and understanding the adsorption process to remove phosphate is vital for the prevention of eutrophication in lakes. In this study, quantum chemical calculations were used to simulate the adsorption of phosphate on variably charged Al-(hydr)oxide, taking into account both explicit and implicit solvation. The corresponding adsorption reactions were modeled via ligand exchange between phosphate species and surface functional groups ($-H_2O/-OH^-$). Gibbs free energies of phosphate adsorption, for inner and outer sphere complexes, using three different simulated pH conditions (acidic, intermediate, and basic) were estimated. The theoretical results indicate that the thermodynamic favorability of phosphate adsorption on Al-(hydr)oxide is directly related to pH. At intermediate pH condition, H-bonded and MM_1 complexes present the most thermodynamically favorable mode of adsorption with –126.2 kJ/mol and –107.8 kJ/mol, respectively. At high pH, simulated IR spectra show that the values of P–O and P–OH stretching modes shifted to higher frequencies with respect to those at low pH.

Keywords: Al-(hydr)oxide; Adsorption; Phosphate; DFT; pH; Gibbs free energy; Wastewater, IR

1. Introduction

Phosphorus is industrially used as both fertilizer and detergent. The residuals are usually dumped into lakes, creeks, and rivers. This over-abundance of phosphorus causes excessive growth of both aquatic plant-life and algae, and depletes the dissolved oxygen supply in the water [1–5]. The high concentration of phosphate in wastewater deteriorates natural aquatic environments and is responsible for the eutrophication of rivers and lakes [6–10]. This problem has brought the attention of authorities concerned about the water quality, resulting in regulations to control the concentration of phosphate in water [11–14].

Adsorption methods have proven to be an attractive solution for phosphate removal due to their operational simplicity, low cost, and excellent kinetic performance [2,15]. However, the low selectivity of the adsorbents in the presence of competing anions (e.g., sulphate, chloride or bicarbonate) and the gradual loss in its capacity, creates the needs to develop and identify adsorbents with high selectivity towards phosphate ion [3,14]. It has been demonstrated that some transition metals with hard Lewis acid properties dispersed on chelating resins present a high selectivity towards phosphate [14,16–20].

Gibbsite is an aluminium hydroxide with a high surface area and constitutes an important adsorbent of anions. The adsorption of phosphate on aluminium hydroxides and oxides has been the subject of intense study for decades [21–23]. The affinity of phosphate for aluminium oxides depends on the phosphate's complexing capacity, which

---

* Corresponding author.

controls the binding process with strong ligand sorption of HPO_4^{2-} and $H_2PO_4^-$ through the formation of inner sphere complexes [13,24–26], and the attractive or repulsive electrostatic field of the charged surface. This mechanism has been proposed for adsorption of arsenate, where using extended X-ray absorption fine structure (EXAFS) spectroscopy confirmed that this anion is selectively bound to the oxide surface through formation of inner and outer sphere complexes [27,28].

It is a well-known experimental fact that the adsorption of phosphate on metal-(hydr)oxide at different pH takes place through inner and outer sphere complexes [29,30]. However, determining the thermodynamic feasibility of either complex it is not easily measured in experimental set-ups. Moreover, for outer sphere complexes, it is not possible to determine these structures through experimental methods. For this reason, computational methods have become a useful tool to study such complexes.

Density Functional Theory (DFT) has been used to calculate the energetic data and adsorption structures of ions on mineral surfaces [31–33]. For example, Guangzhi et al. [34] examined the pH influence on the arsenate adsorption on titanium oxide surfaces. Paul et al. [32] estimated relative Gibbs free energies of sulfate adsorption on variably charged Al- and Fe-(hydr)oxide clusters. They found that the thermodynamic favorability for surface complexation is directly related to the pH conditions on the surfaces of these oxides.

Computational characterizing of the adsorption process of phosphate on Al-hydr(oxide) is of fundamental importance to understand its experimental behavior. In this paper, DFT simulations were used to investigate the thermodynamic favorability for the formation of different phosphate surface complexes, under different pH conditions on Al-(hydr)oxide. Calculated IR frequencies were used to identify important IR-active frequencies to compare with observed peaks.

2. Theoretical methods

In this work, Al-(hydr)oxide clusters resembling those shown by Paul et al. [32] were simulated. These clusters are structurally defined by two aluminum atoms in octahedral coordination with 10 oxygen atoms. This simplification yields a good reproduction of observed vibrational frequencies for surface complexes on a variety of Al minerals; however, more specific models can be created to mimic particular mineral surfaces [35]. Periodic models may represent surfaces more realistically, nevertheless the calculated vibrational frequencies and interatomic distances (as compared with IR/Raman and EXAFS) have not yet proven to be superior compared with molecular cluster models [36]. Furthermore, current work on calculated Gibbs free energies of adsorption suggests that the molecular cluster approach can predict thermodynamics with reasonable accuracy [34–36].

To simulate pH effects, charges on each cluster were varied by adjusting the ratio of functional groups –OH^-/H_2O– (i.e., changing the number of H^+ in the model), that leads to changes in charges of Al-(hydr)oxide in the range +2 to 0. Gibbs free energies of phosphate adsorption were estimated for inner (monodentate and bidentate) and outer (H-bonded) sphere complexes by using stoichiometrically balanced equations. Full optimization of every system was carried out at the DFT level of theory using the B3LYP hybrid functional and the 6–31+g(d,p) basis set on O, H, P and Al atoms. The local minima of the potential energy were verified by frequency calculations on each model structure (i.e., no imaginary frequencies). Frequencies were scaled by a factor of 0.9614 to correct for systematic errors [37].

To account for solvation effects, results are reported using both short-range explicit hydration (six water molecules around each cluster in gaseous phase) and long-range implicit hydration (Integral Equation Formalism Polarized Continuum Model, IEFPCM), which accounts for ion-dipole and dipole-dipole interactions not obtained with explicit solvation of H_2O molecules. This "supermolecule" approach, where species are surrounded by a shell of H_2O and a dielectric continuum has been shown to be an effective method for modeling the effects of water on calculated reaction energies [38]. All calculations were carried out with the Gaussian 09 software [39].

3. Results and discussion

3.1. Thermodynamic adsorption

3.1.1. Inner sphere complexes

The adsorption of phosphate as inner sphere complexes may occur as monodentate mononuclear (MM) or bidentate binuclear (BB) complexes. Fig. 1 shows the formation of BB complex under acidic pH conditions. The $H_2PO_4^-$ anion was used in this work because it is the most abundant species of

$[Al_2(OH)_4(H_2O)_6 \cdot (H_2O)_6]^{2+}$ + $[H_2PO_4(H_2O)_9]^-$ $\longrightarrow$ $[Al_2(OH)_4(H_2O)_4 PO_2 (OH)_2 \cdot (H_2O)_6]^{1+}$ + $11 H_2O$
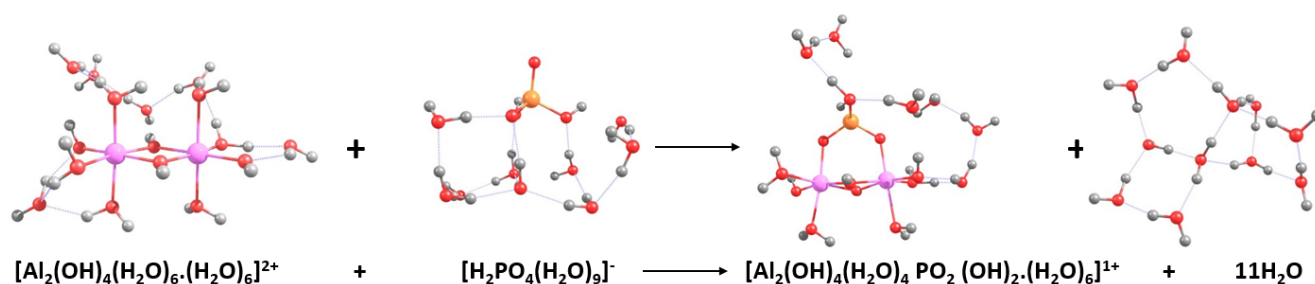
Fig. 1. Adsorption of phosphate as bidentate complex on Al-(hydr)oxide under acidic pH conditions.
Note: The adsorption Gibbs energy is calculated as the energy difference between products and reagents. Red, pink, orange, and gray denote O, Al, P and H atoms, respectively.

$H_nPO_4^{3-n}$ under experimental conditions (wastewater, pH 5.5–6.5) [15]. From speciation distribution diagrams of phosphate, at pH 4, the fraction of $H_2PO_4^-$ is 98.5%, and at pH 6, it is 94.1% [40]. Chubar et al. [7] have suggested that the $H_2PO_4^-$ species were more easily adsorbed on metal (hydr) oxide surfaces than HPO_4^{2-} species. The adsorption of $H_2PO_4^-$ as inner sphere complexes occurs via ligand exchange with surface functional groups (–H_2O or –OH^-) and is a function of pH, surface charge and structure [16,34].

A ligand exchange mechanism suggests that at low pH, reactive surface groups are protonated, and $H_2PO_4^-$ exchanges with two H_2O (Fig. 1). At intermediate pH, a mixture of reactive surface groups (–H_2O and –HO^-) may coexist, and $H_2PO_4^-$ exchanges with either –HO^- or –H_2O. At higher pH, $H_2PO_4^-$ exchanges only with –HO^- functional groups. Similar mechanisms are proposed for adsorption oxyanions on metal-(hydr)oxides [41]. During the adsorption process, MM and BB complexes may coexist as follows: when a $H_2PO_4^-$ molecule approaches the Al-(hydr)oxide, it would first exchange with either a –H_2O or –OH functional group to form a MM complex, leading to phosphate being adsorbed to the surface group with one coordinating number. Then, the $H_2PO_4^-$ group continues to react with an adjacent surface group and releases either the –H_2O or OH^- functional group to form a BB complex, which needs double-coordinated adsorption sites. It should be noted that it is possible to find both BB and MM complexes regardless of the pH condition; furthermore, in experimental tests all these adsorption modes can be found. Therefore, knowledge of the thermodynamic

feasibility and vibrational frequencies of the adsorption processes is a fundamental aspect in understanding these adsorption pathways.

Knowledge of calculated vibrational frequencies allows to find direct correlations between experimental and theoretical values. Comparison between measured and predicted multi-peaked spectral features makes it possible to assign surface complexes to experimental spectra in a precise and reliable way. Although calculated adsorption energies (ΔG_{ads}) are not expected to output highly accurate absolute energies (compared to the experiment) they allow to predict which species are the most favorable from a thermodynamic point of view.

The calculation of Gibbs free energy of adsorption (ΔG_{ads}) was applied to all complexes under the three simulated pH conditions (i.e., acidic, intermediate and basic). Fig. 2 shows the adsorption complexes under intermediate pH conditions (all complexes under acidic and basic pH are found in supplementary material, Figs. S1 and S2). The reactants and products used to calculate the adsorption reaction (ΔG_{ads}) are shown in Table 1. Table 2 shows the balanced equations used to estimate the adsorption Gibbs energies for phosphate on Al-(hydr)oxide under different pH conditions.

Table 2 shows that BB adsorption is exergonic with an energy of –90.1 kJ/mol and –72.5 kJ/mol under acidic and intermediate pH conditions, respectively. At basic pH conditions, the adsorption for phosphate is unfavorable +33.7 kJ/mol. According to these results, the adsorption as BB complex for phosphate is favored with an energy difference of 17.6 kJ/mol under acidic pH conditions. In order to study the

$[Al_2(OH)_5(H_2O)_5.(H_2O)_6]^+$

BB: $[Al_2(OH)_4(H_2O)_4PO_2(OH)_2.(H_2O)_6]^{+1}$

MM_1:$[Al_2(OH)_5(H_2O)_4PO_2(OH)_2.(H_2O)_6]^0$

MM_2:$[Al_2(OH)_4(H_2O)_5PO_2(OH)_2.(H_2O)_6]^{+1}$

H-Bond : $[Al_2(OH)_5(H_2O)_5PO_2(OH)_2.(H_2O)_6]^0$
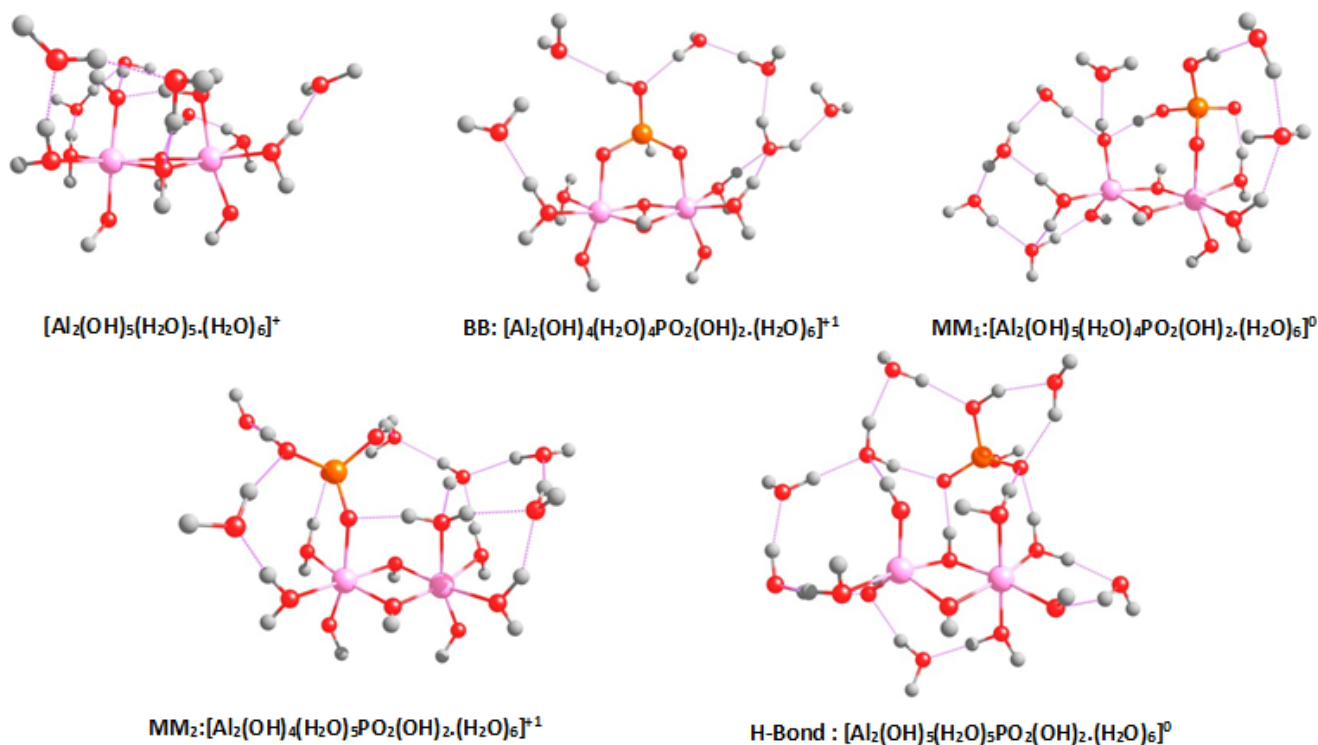
Fig. 2. DFT-calculated structures of inner-sphere and H-bond adsorption products of phosphate on Al-(hydr)oxide under intermediate pH conditions.
Note: Red, pink, orange, and gray spheres denote O, Al, P and H atoms, respectively. MM_1: Monodentate mononuclear complex bonded to one H_2O surface functional group with one OH group in the adjacent surface site and MM_2: Monodentate mononuclear complex bonded to one OH surface functional group with one H_2O group in the adjacent surface site.

Table 1
Reactant and product energies calculated for each species in the phosphate adsorption on different charged Al-(hydr)oxides

Reaction species	E_{gas}	E_{IEFPCM}	G_{IEFPCM}	H_{IEFPCM}	Thermal correction G_{IEFPCM}
$[H_2PO_4(H_2O)_9]^-$	–1,331.4721	–1,331.5579	–1,331.6172	–1,331.5290	0.2040
$11H_2O$	–840.6634	–840.6999	–840.7561	–840.6736	0.2151
$10H_2O$	–764.2349	–764.2680	–764.3218	–764.2435	0.1926
$9H_2O$	–687.8052	–687.8348	–687.8863	–687.8126	0.1694
$OH^-(H_2O)_{10}$	–840.1531	–840.2392	–840.2955	–840.2122	0.2047
$OH^-(H_2O)_9$	–763.7262	–763.8119	–763.8632	–763.7874	0.1856
$(OH^-)_2(H_2O)_9$	–839.5176	–839.7641	–839.8194	–839.7373	0.1926
Surface Clusters					
[a]$[Al_2(OH)_4(H_2O)_6 \cdot (H_2O)_6]^{2+}$	–1,705.1485	–1,705.3786	–1,705.4445	–1,705.3395	0.2979
[b]$[Al_2(OH)_5(H_2O)_5 \cdot (H_2O)_6]^+$	–1,704.8554	–1,704.9408	–1,705.0018	–1,704.9059	0.2895
[c]$[Al_2(OH)_6(H_2O)_4 \cdot (H_2O)_6]^0$	–1,704.4501	–1,704.4931	–1,704.5572	–1,704.4567	0.2750
Bidentate Binuclear Complex (BB)					
$[Al_2(OH)_4(H_2O)_4PO_2(OH)_2 \cdot (H_2O)_6]^{2+}$	–2,196.1685	–2,196.2616	–2,196.3304	–2,196.2216	0.2772
	–2,196.1719	–2,196.2623	–2,196.3368	–2,196.2202	0.2744
	–2,196.1775	–2,196.2639	–2,196.3347	–2,196.2242	0.2789
Monodentate Mononuclear Complexes (MM)					
[a]$[Al_2(OH)_4(H_2O)_5PO_2(OH)_2 \cdot (H_2O)_6]^{1+}$	–2,272.5976	–2,272.6899	–2,272.7626	–2,272.6473	0.3028
[b]$MM_1[Al_2(OH)_5(H_2O)_4PO_2(OH)_2 \cdot (H_2O)_6]^0$	–2,272.2172	–2,272.2621	–2,272.3319	–2,272.2217	0.2946
[b]$MM_2[Al_2(OH)_4(H_2O)_5PO_2(OH)_2 \cdot (H_2O)_6]^{+1}$	–2,272.6032	–2,272.6899	–2,272.7622	–2,272.6474	0.3024
[c]$[Al_2(OH)_5(H_2O)_4PO_2(OH)_2 \cdot (H_2O)_6]^0$	–2,272.2545	–2,272.2388	–2,272.3065	–2,272.1987	0.2952
H-Bonded Complexes					
[a]$[Al_2(OH)_4(H_2O)_6PO_2(OH)_2 \cdot (H_2O)_6]^{+1}$	–2,349.0417	–2,349.1322	–2,349.2050	–2,349.0898	0.3259
[b]$[Al_2(OH)_5(H_2O)_5PO_2(OH)_2 \cdot (H_2O)_6]^0$	–2,348.6492	–2,348.6953	–2,348.7714	–2,348.6516	0.3147

Note: All calculations were done using a B3LYP theory level and a 6–31+g(d,p) basis set on O, H, P and Al.
[a]From the optimized structure at simulated acidic pH.
[b]From the optimized structure at simulated intermediate pH.
[c]From the optimized structure at simulated basic pH. MM_1: Monodentate mononuclear phosphate bonded to one H_2O surface functional group with an OH group in the adjacent surface site. MM_2: Monodentate mononuclear phosphate bonded to one OH surface functional group with a H_2O group in the adjacent surface site.

Table 2
Calculated Gibbs adsorption energy (ΔG_{ads}) (kJ/mol) of phosphate on various protonated Al-(hydr)oxide clusters

pH	Adsorption reaction equations	ΔG_{ads} (kJ/mol)
	Bidentade binuclear complexes (BB)	
Acidic	$H_2PO_4^-(H_2O)_9 + Al_2(OH)_4(H_2O)_6 \cdot (H_2O)_6]^{2+} \rightarrow [Al_2(OH)_4(H_2O)_4 PO_2(OH)_2 \cdot (H_2O)_6]^{1+} + 11H_2O$	–90.12
Intermediate	$H_2PO_4^-(H_2O)_9 + [Al_2(OH)_5(H_2O)_5 \cdot (H_2O)_6]^{1+} \rightarrow [Al_2(OH)_4(H_2O)_4PO_2(OH)_2 \cdot (H_2O)_6]^{1+} + OH^-(H_2O)_{10}$	–72.47
Basic	$H_2PO_4^-(H_2O)_9 + [Al_2(OH)_6(H_2O)_4 \cdot (H_2O)_6]^0 \rightarrow [Al_2(OH)_4(H_2O)_4PO_2(OH)_2 \cdot (H_2O)_6]^{1+} + (OH^-)_2(H_2O)_9$	33.71
	Monodentate Mononuclear Complexes (MM)	
Acid	$H_2PO_4^-(H_2O)_9 + [Al_2(OH)_4(H_2O)_6 \cdot (H_2O)_6]^{2+} \rightarrow [Al_2(OH)_4(H_2O)_5PO_2(OH)_2 \cdot (H_2O)_6]^{1+} + 10 H_2O$	–76.78
Intermediate	$H_2PO_4^-(H_2O)_9 + [Al_2(OH)_5(H_2O)_5 \cdot (H_2O)_6]^{1+} \rightarrow [Al_2(OH)_5(H_2O)_4PO_2(OH)_2 \cdot (H_2O)_6]^0 + 10H_2O$	–107.79
	$H_2PO_4^-(H_2O)_9 + [Al_2(OH)_5(H_2O)_5 \cdot (H_2O)_6]^{1+} \rightarrow [Al_2(OH)_4(H_2O)_5PO_2(OH)_2 \cdot (H_2O)_6]^{+1} + OH(H_2O)_9$	–30.93
Basic	$H_2PO_4^-(H_2O)_9 + [Al_2(OH)_6(H_2O)_4 \cdot (H_2O)_6]^0 \rightarrow [Al_2(OH)_5(H_2O)_4PO_2(OH)_2 \cdot (H_2O)_6]^0 + (OH^-)(H_2O)_9$	17.30
	H-Bond Complexes	
Acid	$H_2PO_4^-(H_2O)_9 + [Al_2(OH)_4(H_2O)_6 \cdot (H_2O)_6]^{2+} \rightarrow [Al_2(OH)_4(H_2O)_6 PO_2(OH)_2 \cdot (H_2O)_6]^{1+} + 9H_2O$	–94.93
Intermediate	$H_2PO_4^-(H_2O)_9 + [Al_2(OH)_5(H_2O)_5 \cdot (H_2O)_6]^{1+} \rightarrow [Al_2(OH)_5(H_2O)_5 PO_2(OH)_2 \cdot (H_2O)_6]^0 + 9H_2O$	–126.17

influence of an adjacent surface site (–H_2O or –OH^-) to form MM complexes, two adsorption processes were calculated: MM_1 and MM_2 complexes. In MM_1, phosphate is bonded to one –H_2O surface functional group with an –OH^- group in the adjacent surface site. In contrast, for MM_2, phosphate is bonded to an –OH^- surface functional group with a –H_2O group in the adjacent surface site. Both types of complexes can be found under intermediate pH conditions. ΔG_{ads} energies showed that in clusters of Al-(hydr)oxide, where both –H_2O and –OH^- surface functional groups coexisted on two adjacent sites (e.g., intermediate pH condition), phosphate preferred to react with the labile –H_2O surface group to form MM_1 complexes (–107.8 kJ/mol), instead of the stable –OH^- surface group to form MM_2 complexes (–31.0 kJ/mol). Under basic pH conditions, adsorption of phosphate on Al-(hydr) oxide was predicted to be endergonic (+17.3 kJ/mol). These ΔG_{ads} energies thus show that for phosphate, the reaction with a labile group (–H_2O, low pH conditions) is much easier than with a stable group (–OH^-, high pH condition) and that the lability of the surface functional group affects the adsorption energy. In this adsorption process, the most favorable inner sphere complex was MM_1 whose energy is ~ 1.2 times higher than BB complex under acidic pH. These results suggest that acidic and intermediate pH are optimal pH conditions to have a good adsorption of phosphate when using Al-(hydr) oxide. It is important to emphasize here that our results suggest that, at intermediate pH conditions, the MM1 complex is the most thermodynamically favorable result. Moreover, in basic pH conditions we found none of the complexes is energetically feasible, which is in agreement with results reported elsewhere [22,23].

Although our study is devoted to Al-(hydr)oxide, it is also important to mention that a straightforward extension can be made to include Fe. Indeed, we have previously reported on the feasibility of phosphate adsorption on Fe-(hydr)oxide, and found that the BB complex is the most thermodynamically favorable complex in acidic pH conditions [16]. We are addressing this result with more detail in an upcoming publication.

3.1.2. Outer sphere complexes

The outer-sphere complex (H-bonded) may be described as an electrostatic attraction between positively charged Al-(hydr)oxide and negatively charged phosphate without release any of the surface functional groups (–H_2O or –OH^-) [20,40,41]. The adsorption of H-bond complex was predicted to be exergonic with an energy of –94.9 kJ/mol and –126.2 kJ/mol under acidic and intermediate pH conditions, respectively. This high thermodynamic favorability can be explained by the formation of assisted charged hydrogen bonds between phosphate anion and the functional groups –H_2O/–OH^- on the surface of Al-(hydr)oxide.

With the results showed above, it can be concluded that during phosphate adsorption on Al-(hydr)oxide, under acidic and intermediate pH conditions, it is possible to find a mixture of inner and outer sphere complexes, dominated by H-bonded, MM_1 and BB. The mixture of complexes makes it difficult to characterize in experiments (e.g., vibrational frequencies and bond lengths); therefore, computational chemistry becomes a valuable tool to study these adsorption modes.
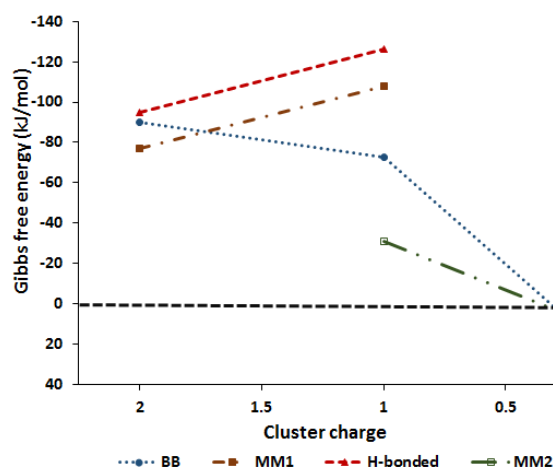
Fig. 3. Gibbs free energies of phosphate adsorption on various protonated Al-(hydr)oxide clusters.
Note: The horizontal coordinate represents the reactant cluster charge, which is a proxy for the pH conditions (see text). Different line-types correspond to different complexes, MM_1 and MM_2 correspond to the MM complex where the phosphate bonded to a H_2O or OH^- surface functional groups, respectively.

Adsorption energy curves for phosphate (Fig. 3) showed that the thermodynamic feasibility of inner-sphere and outer-sphere adsorption was directly related to pH conditions. For Al-hydr(oxide) the adsorption of phosphate under acidic and intermediate pH was favorable for both inner-sphere and outer-sphere complexes (complexes with negative values of Gibbs energies).

Numerous macroscopic results indicate that with increasing pH, phosphate adsorption on Al-hydr(oxides) sharply decreases [22,23,42,43]. Results presented here qualitatively agree with this experimental observation. Tanada et al. [22] evaluated the removal of phosphate by Al-hydr(oxides) and they found that the amount of phosphate adsorbed at pH=4 was greater than the adsorbed at pH=9. Xu et al. [43] reported that when the initial concentration was 0.64 mM, the percentage removal of phosphate by aluminum-loaded-zeolite decreased from 80% to around 40% at a pH from 2 to 11, respectively. This anti-correlated behavior between surface loading and pH is primarily attributed both to a reduction in positively charged surface sites and increased competition with OH^- adsorption.

The most thermodynamically favorable complexes were, H-bond and MM_1 with adsorption Gibbs energies of –126.2 kJ/mol and –107.8 kJ/mol, respectively, at intermediate pH conditions.

DFT results suggest that in order to get a good adsorption of phosphate on Al-(hydr)oxide it is necessary to work under intermediate pH condition. This pH is more favorable for the adsorption of phosphate as outer sphere (H-bond) and inner sphere (MM_1) complexes. These computational results are in complete agreement with experiments [22,23]. Shin et al. [44] characterize phosphate adsorption on aluminum-impregnated mesoporous silicates using Fourier-Transformed Infrared Spectroscopy (FTIR) and X-ray Photoelectron Spectroscopy (XPS) techniques. They found that during phosphate removal the adsorbent surface

(aluminum oxide) was covered mainly with monodentate surface complexes at equilibrium. This large fraction of monodentate surface complexes during the adsorption process explains the increase of adsorption capacity on Al-adsorbent. When MM surface complexes are formed, the stoichiometry between phosphates and surface –H_2O or –OH^- groups is one-to-one, while for BB complexes, phosphate has to react with two surfaces: –H_2O or –OH^- groups. Accordingly, monodentate adsorption is more efficient in the removal of phosphate from water.

3.2. Vibrational analysis

Due to both the similarity between P and As oxoanions and the lack of EXAFS studies of phosphate on gibbsite, our theoretical data for P–Al and P–O bond distances in MM and BB complexes of phosphate on Al-(hydr)oxide can be compared with the experimental data collected by Ladeira et al. [45] for the adsorption of arsenate (As) on Gibbsite. The (experimentally) measured distance for As–Al between oxoanions and the gibbsite is 3.19 Å, whereas the theoretical value was estimated in our calculations to be 3.15 Å for

P–Al. Another bond distance that can be compared directly with EXAFS results is the As–O interaction, in this case the measured value is 1.68 Å, and the calculated is around 1.56 Å for the distance P–O in BB and MM complexes of phosphate on Al-(hydr)oxide. These results validate our methodology and give us strong confidence that our model is a good representation of Al-(hydr)oxide. With the use of EXAFTS, spectroscopy is not possible to determine these bond lengths in outer sphere complexes and, therefore, IR frequencies are the remaining viable option to such complexes.

To investigate phosphate complexes on Al-(hydr)oxide, we first compared IR experimental spectra of adsorbed phosphate on gibbsite [46] with IR calculated spectra for each complex (Figs. 4, S3 and S4). For simplicity, we did not distinguish between symmetric and asymmetric modes. From Figs. 4, S1 and S2, it can be seen that there is not a strong dependence of the IR spectra of the P surface complexes on pH. All the adsorption modes, under all pH conditions, present several frequency values between approximately 800 cm^{-1} and 1250 cm^{-1}. Fig. 4 shows FTIR spectra for phosphate adsorption complexes simulated at intermediate pH conditions. It can be seen that the bands predicted by our theoretical models are in
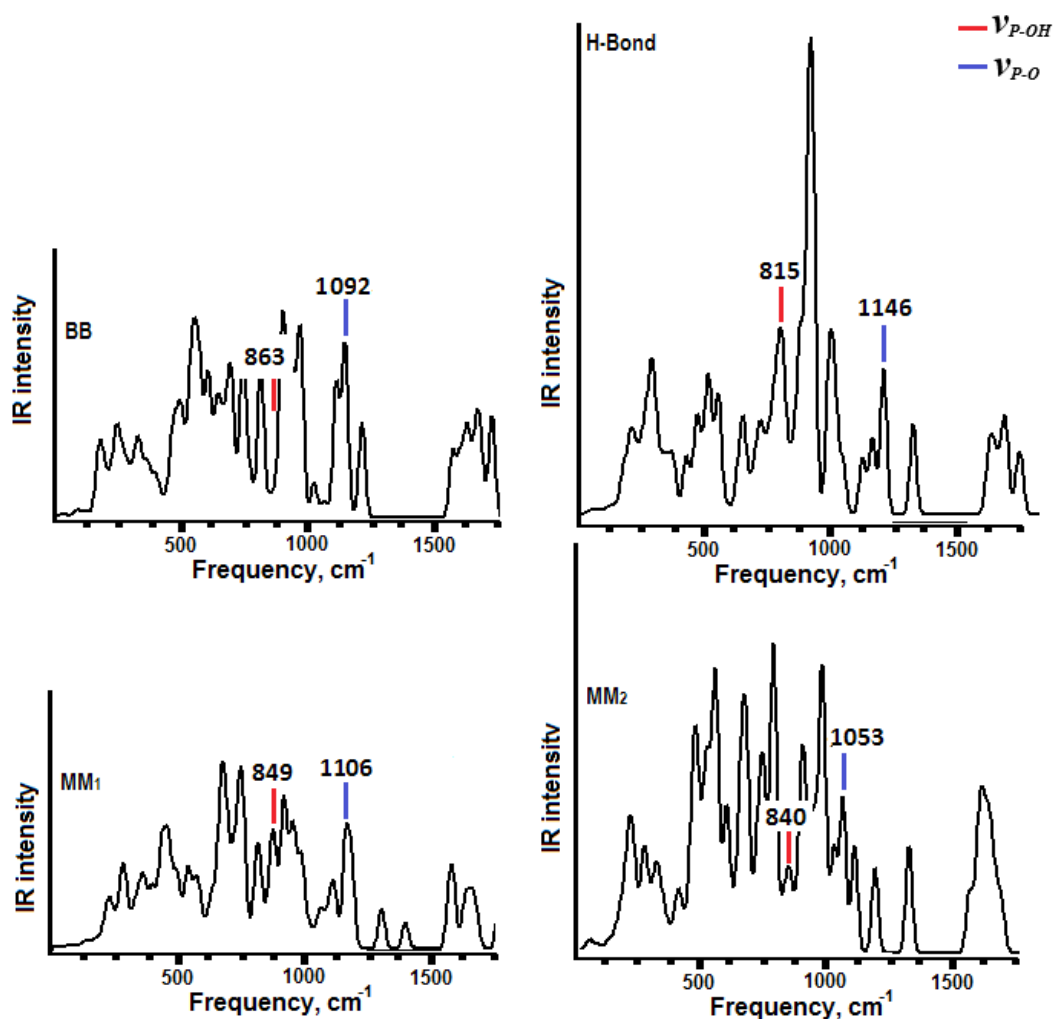
Fig. 4. IR spectra of BB (top-left), H-Bonded (top-right), MM$_1$ (bottom-left) and MM$_2$ (bottom-right) complexes at intermediate pH conditions.
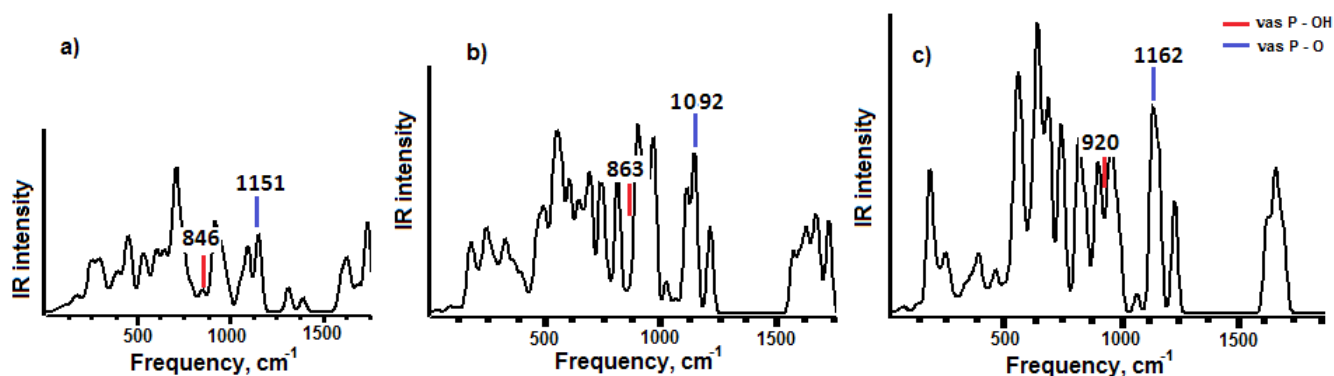
Fig. 5. IR spectra of BB complexes at (a) acidic, (b) intermediate and (c) basic simulated pH conditions.

the range of 815–863 cm^{-1} for the ν_{P-OH} vibrational mode and 1092–1146 cm^{-1} for the ν_{P-O} vibrational mode. These values are in very good agreement with the experimental ones, which are in the range of 821–977 cm^{-1} and 1150–1225 cm^{-1} for the ν_{P-OH} and ν_{P-O}, respectively. From these spectra, it is clear that inner-sphere adsorption of phosphate (BB, MM$_1$ and MM$_2$ complexes) causes the reduction in the vibrational frequency $\nu_{P-O'}$ (1053 cm^{-1}) in comparison to the vibrational frequency $\nu_{P-O'}$ (1146 cm^{-1}) in outer-sphere complexes (H-bonded). This reduction resulted from the coordination of H$_2$PO$_4^-$ with Al-(hydr)oxide, indicating that a bond was created during the formation of inner-sphere complexes, which is consistent with experimental results [46]. The experimental frequency ν_{P-O} in the free anion H$_2$PO$_4^-$ is 1155 cm^{-1} and is very similar to ν_{P-O} of 1146 cm^{-1} in H-bonded complexes. The slight shift could be due to the distortion in adsorbed P molecules as H-bonded complex via van der Waals forces or electrostatic attraction between positively charged Al-(hydr)oxide and H$_2$PO$_4^-$ anion. Identifying this band thus allows us to speculate on the molecular configurations of the surface complexes.

In Figs. 4, S3 and S4, it is also noted that for complexes at basic conditions, the vibrational frequencies ν_{P-O} and ν_{P-OH} have a slight shift toward the right. The vibrational frequencies, ν_{P-O} and ν_{P-OH}, in BB and MM$_2$ complexes under basic pH are in the range 905–920 cm^{-1} and 1162–1231 cm^{-1}, respectively, whereas the same frequencies for BB and MM$_2$ complexes at acidic and intermediate pH are in the range 840–863 cm^{-1} and 1109–1151 cm^{-1}.

This observation is emphasized in Fig. 5; it shows IR spectra for BB complexes obtained at acidic, intermediate and basic pH. The shift to higher values of the vibrational frequencies, ν_{P-O} and ν_{P-OH}, in BB complex under basic pH condition can be easily appreciated. As expected, differences in the bond length reflect changes in the vibrational frequencies: elongated bonds and, therefore, weak bonds correspond to low vibrational frequencies, and vice versa. Therefore, this shifting is related to the greater strength of the Al–P–O bonds involved in the adsorption as BB complex of H$_2$PO$_4^-$ anion on Al-(hydr)oxide at acid and intermediate pH. This increased strength directly creates a weakness in the P–O and P–OH bonds, which in turn generates low values of vibrational frequencies in complexes for acidic and intermediate pH conditions. The high values ν_{P-O} and ν_{P-OH} in BB complexes for basic pH conditions leads to a lower strength in the Al–P–O

bonds involved in the adsorption process. The shift of these frequencies agrees with the thermodynamic data, which indicated that the adsorption as inner-outer sphere complexes is favorable under acidic and intermediate pH conditions and unfavorable under basic pH conditions.

4. Conclusions

Through quantum chemical calculations, it was shown that phosphate adsorption on Al-(hydr)oxide involves both electrostatic interactions (outer-sphere) and chemical bonding (inner-sphere). The thermodynamic feasibility of the inner and outer-sphere adsorption is directly related to the pH. Intermediate and acidic pH conditions favored the adsorption of phosphate as H-bond and MM complexes. IR spectroscopy has been widely used for surface complex studies because it can provide direct structural information. In this work, a good correspondence between the experimental and calculated IR vibrational frequencies was found. Therefore, IR data can provide useful insights into surface complex formation in a way that supplements the experimental data. For example, it can be used to assess whether the adsorption occurs through bidentate, monodentate or H-bonded complexes, showing this way that calculated data are useful in surface complex studies, where experimental interpretation can be ambiguous.

References

[1] M.R. Awual, A. Jyo, Assessing of phosphorus removal by polymeric anion exchangers, Desalination, 281 (2011) 111–117.
[2] M.R. Awual, A. Jyo, T. Ihara, N. Seko, M. Tamada, K.T. Lim, Enhanced trace phosphate removal from water by zirconium(IV) loaded fibrous adsorbent, Water Res., 45 (2011) 4592–4600.
[3] B.K. Biswas, K. Inoue, K.N. Ghimire, H. Harada, K. Ohto, H. Kawakita, Removal and recovery of phosphorus from water by means of adsorption onto orange waste gel loaded with zirconium, Bioresour, Technol., 99 (2008) 8685–8690.
[4] I. Midorikawa, H. Aoki, A. Omori, T. Shimizu, Y. Kawaguchi, K. Kassai, T. Murakami, Recovery of high purity phosphorus from municipal wastewater secondary effluent by a high-speed adsorbent, Water Sci. Technol., 58 (2008) 1601–1607.

[5] X. Zhu, A. Jyo, Column-mode phosphate removal by a novel highly selective adsorbent, Water Res., 39 (2005) 2301–2308.

[6] N.Y. Acelas, E. Flórez, D. López, Phosphorus recovery through struvite precipitation from wastewater: effect of the competitive ions, Desal. Water Treat., 54 (2015) 2468–2479.

[7] N.I. Chubar, V.A. Kanibolotskyy, V.V. Strelko, G.G. Gallios, V.F. Samanidou, T.O. Shaposhnikova, V.G. Milgrandt, I.Z. Zhuravlev, Adsorption of phosphate ions on novel inorganic ion exchangers, Colloids Surf. A: Physicochem. Eng. Asp., 255 (2005) 55–63.

[8] A. Genz, A. Kornmüller, M. Jekel, Advanced phosphorus removal from membrane filtrates by adsorption on activated aluminium oxide and granulated ferric hydroxide, Water Res., 38 (2004) 3523–3530.

[9] Y. Jaffer, T.A. Clark, P. Pearce, S.A. Parsons, Potential phosphorus recovery by struvite formation, Water Res., 36 (2002) 1834–1842.

[10] A.D. Kney, D. Zhao, A pilot study on phosphate and nitrate removal from secondary wastewater effluent using a selective ion exchange process, Environ. Technol., 25 (2004) 533–542.

[11] F.E.F. Act, Florida State Legislature, Tallahassee, Florida, 1994.

[12] M.R. Awual, A. Jyo, S.A. El-Safty, M. Tamada, N. Seko, A weak-base fibrous anion exchanger effective for rapid phosphate removal from water, J. Hazard Mater., 188 (2011) 164–171.

[13] L.M. Blaney, S. Cinar, A.K. SenGupta, Hybrid anion exchanger for trace phosphate removal from water and wastewater, Water Res., 41 (2007) 1603–1613.

[14] D. Zhao, A.K. Sengupta, Ultimate removal of phosphate from wastewater using a new class of polymeric ion exchangers, Water Res., 32 (1998) 1613–1625.

[15] N.Y. Acelas, B.D. Martin, D. López, B. Jefferson, Selective removal of phosphate from wastewater using hydrated metal oxides dispersed within anionic exchange media, Chemosphere, 119 (2015) 1353–1360.

[16] N.Y. Acelas, S.M. Mejia, F. Mondragón, E. Flórez, Density functional theory characterization of phosphate and sulfate adsorption on Fe-(hydr)oxide: reactivity, pH effect, estimation of Gibbs free energies, and topological analysis of hydrogen bonds, Comp. Theor. Chem., 1005 (2013) 16–24.

[17] A.O. Babatunde, Y.Q. Zhao, Y. Yang, P. Kearney, Reuse of dewatered aluminium-coagulated water treatment residual to immobilize phosphorus: batch and column trials using a condensed phosphate, Chem. Eng. J., 136 (2008) 108–115.

[18] K. Kuzawa, Y.-J. Jung, Y. Kiso, T. Yamada, M. Nagai, T.-G. Lee, Phosphate removal and recovery with a synthetic hydrotalcite as an adsorbent, Chemosphere, 62 (2006) 45–52.

[19] S.I. Lee, S.Y. Weon, C.W. Lee, B. Koopman, Removal of nitrogen and phosphate from wastewater by addition of bittern, Chemosphere, 51 (2003) 265–271.

[20] R.S.S. Wu, K.H. Lam, J.M.N. Lee, T.C. Lau, Removal of phosphate from water by a highly selective La(III)-chelex resin, Chemosphere, 69 (2007) 289–294.

[21] Y.S.R. Chen, J.N. Butler, W. Stumm, Kinetic study of phosphate reaction with aluminum oxide and kaolinite, Environ. Sci. Technol., 7 (1973) 327–332.

[22] S. Tanada, M. Kabayama, N. Kawasaki, T. Sakiyama, T. Nakamura, M. Araki, T. Tamura, Removal of phosphate by aluminum oxide hydroxide, J. Colloid Interface Sci., 257 (2003) 135–140.

[23] W.H. van Riemsdijk, J. Lyklema, Reaction of phosphate with gibbsite (Al(OH)3) beyond the adsorption maximum, J. Colloid Interface Sci., 76 (1980) 55–66.

[24] P.K. Dutta, A.K. Ray, V.K. Sharma, F.J. Millero, Adsorption of arsenate and arsenite on titanium dioxide suspensions, J. Colloid Interface Sci., 278 (2004) 270–275.

[25] S. Sengupta, A. Pandit, Selective removal of phosphorus from wastewater combined with its recovery as a solid-phase fertilizer, Water Res., 45 (2011) 3318–3330.

[26] T.M. Suzuki, J.O. Bomani, H. Matsunaga, T. Yokoyama, Preparation of porous resin loaded with crystalline hydrous zirconium oxide and its application to the removal of arsenic, React. Funct. Polym., 43 (2000) 165–172.

[27] L. Cumbal, A.K. SenGupta, Arsenic removal using polymer-supported hydrated iron(III) oxide nanoparticles: role of Donnan membrane effect, Environ. Sci. Technol., 39 (2005) 6508–6515.

[28] B.A. Manning, S.E. Fendorf, S. Goldberg, Surface structures and stability of arsenic(III) on goethite: spectroscopic evidence for inner-sphere complexes, Environ. Sci. Technol., 32 (1998) 2383–2388.

[29] P. Persson, N. Nilsson, S. Sjöberg, Structure and bonding of orthophosphate ions at the iron oxide–aqueous interface, J. Colloid Interface Sci., 177 (1996) 263–275.

[30] M.I. Tejedor-Tejedor, M.A. Anderson, The protonation of phosphate on the surface of goethite as studied by CIR-FTIR and electrophoretic mobility, Langmuir, 6 (1990) 602–611.

[31] K.W. Paul, M.J. Borda, J.D. Kubicki, D.L. Sparks, Effect of dehydration on sulfate coordination and speciation at the Fe-(hydr)oxide-water interface: a molecular orbital/density functional theory and Fourier transform infrared spectroscopic investigation, Langmuir, 21 (2005) 11071–11078.

[32] K.W. Paul, J.D. Kubicki, D.L. Sparks, Quantum chemical calculations of sulfate adsorption at the Al– and Fe-(hydr) oxide-H_2O interface estimation of Gibbs free energies, Environ. Sci. Technol., 40 (2006) 7717–7724.

[33] D.M. Sherman, S.R. Randall, Surface complexation of arsenic(V) to iron(III) (hydr)oxides: structural mechanism from ab initio molecular geometries and EXAFS spectroscopy, Geochim. Cosmochim. Acta, 67 (2003) 4223–4230.

[34] G. He, M. Zhang, G. Pan, Influence of pH on initial concentration effect of arsenate adsorption on TiO_2 surfaces: thermodynamic, DFT, and EXAFS interpretations, J. Phys. Chem. C, 113 (2009) 21679–21686.

[35] J.D. Kubicki, S.E. Apitz, Molecular cluster models of aluminum oxide and aluminum hydroxide surfaces, Am. Mineral., 83 (1998) 1054–1066.

[36] K.W. Paul, J.D. Kubicki, D.L. Sparks, Sulphate adsorption at the Fe-(hydr)oxide-H2O interface: comparison of cluster and periodic slab DFT predictions, Eur. J. Soil. Sci., 58 (2007) 978–988.

[37] A.P. Scott, L. Radom, Harmonic vibrational frequencies: an evaluation of Hartree−Fock, Møller−Plesset, quadratic configuration interaction, density functional theory, and semiempirical scale factors, J. Phys. Chem., 100 (1996) 16502–16513.

[38] T.A. Keith, M.J. Frisch, Inclusion of Explicit Solvent Molecules in a Self-Consistent-Reaction Field Model of Solvation, Modeling the Hydrogen Bond, American Chemical Society, 1994, pp. 22–35.

[39] M.J. Frisch, G.W. Trucks, H.B. Schlegel, G.E. Scuseria, M.A. Robb, J.R. Cheeseman, J.A. Montgomery, Jr., T. Vreven, K.N. Kudin, J.C. Burant, J.M. Millam, S.S. Iyengar, J. Tomasi, V. Barone, B. Mennucci, M. Cossi, G. Scalmani, N. Rega, G.A. Petersson, H. Nakatsuji, M. Hada, M. Ehara, K. Toyota, R. Fukuda, J. Hasegawa, M. Ishida, T. Nakajima, Y. Honda, O. Kitao, H. Nakai, M. Klene, X. Li, J.E. Knox, H.P. Hratchian, J.B. Cross, V. Bakken, C. Adamo, J. Jaramillo, R. Gomperts, R.E. Stratmann, O. Yazyev, A.J. Austin, R. Cammi, C. Pomelli, J.W. Ochterski, P.Y. Ayala, K. Morokuma, G.A. Voth, P. Salvador, J.J. Dannenberg, V.G. Zakrzewski, S. Dapprich, A.D. Daniels, M.C. Strain, O. Farkas, D.K. Malick, A.D. Rabuck, K. Raghavachari, J.B. Foresman, J.V. Ortiz, Q. Cui, A.G. Baboul, S. Clifford, J. Cioslowski, B.B. Stefanov, G. Liu, A. Liashenko, P. Piskorz, I. Komaromi, R.L. Martin, D.J. Fox, T. Keith, M.A. Al-Laham, C.Y. Peng, A. Nanayakkara, M. Challacombe, P.M.W. Gill, B. Johnson, W. Chen, M.W. Wong, C. Gonzalez, and J.A. Pople, Gaussian 09, Revision C.02, Gaussian Inc., Wallingford, CT, 2004.

[40] X. Yang, D. Wang, Z. Sun, H. Tang, Adsorption of phosphate at the aluminum (hydr)oxides-water interface: role of the surface acid-base properties, Colloids Surf. A: Physicochem. Eng. Asp., 297 (2007) 84–90.

[41] G. He, G. Pan, M. Zhang, Studies on the reaction pathway of arsenate adsorption at water–TiO_2 interfaces using density functional theory, J. Colloid Interface Sci., 364 (2011) 476–481.

[42] I.C. Regelink, L. Weng, G.J. Lair, R.N.J. Comans, Adsorption of phosphate and organic matter on metal (hydr)oxides in arable and forest soil: a mechanistic modelling study, Eur. J. Soil. Sci., 66 (2015) 867–875.

[43] Y.H. Xu, A. Ohki, S. Maeda, Removal of arsenate, phosphate, and fluoride ions by aluminium-loaded shirasu-zeolite, Toxicol. Environ. Chem., 76 (2000) 111–124.

[44] E.W. Shin, J.S. Han, M. Jang, S.-H. Min, J.K. Park, R.M. Rowell, Phosphate adsorption on aluminum-impregnated mesoporous silicates: surface structure and behavior of adsorbents, Environ. Sci. Technol., 38 (2004) 912–917.

[45] A.C.Q. Ladeira, V.S.T. Ciminelli, H.A. Duarte, M.C.M. Alves, A.Y. Ramos, Mechanism of anion retention from EXAFS and density functional calculations: arsenic (V) adsorbed on gibbsite, Geochim. Cosmochim. Acta, 65 (2001) 1211–1217.

[46] C.V. Luengo, N.J. Castellani, R.M. Ferullo, Quantum chemical study on surface complex structures of phosphate on gibbsite, Spectrochim. Acta A: Mol. Biomol. Spectrosc., 147 (2015) 193–199.

Supplementary data

Optimized geometries
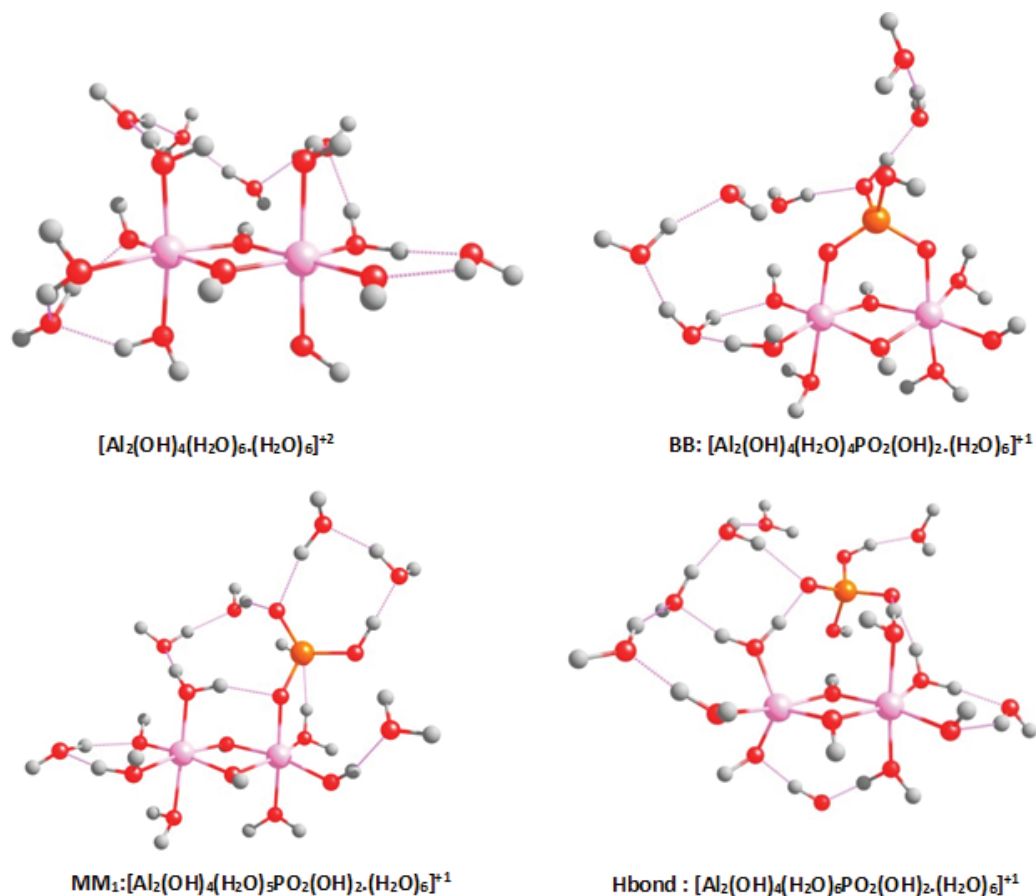
$[Al_2(OH)_4(H_2O)_6.(H_2O)_6]^{+2}$

BB: $[Al_2(OH)_4(H_2O)_4PO_2(OH)_2.(H_2O)_6]^{+1}$

MM_1: $[Al_2(OH)_4(H_2O)_5PO_2(OH)_2.(H_2O)_6]^{+1}$

Hbond : $[Al_2(OH)_4(H_2O)_6PO_2(OH)_2.(H_2O)_6]^{+1}$

Fig. S1. DFT calculated structures of inner-sphere and H-bond adsorption products of phosphate on Al-(hydr)oxide under acidic pH conditions.
Note: Red, pink, orange and gray denote O, Al, P, and H atoms, respectively.

$[Al_2(OH)_6(H_2O)_4.(H_2O)_6]^0$

BB: $[Al_2(OH)_4(H_2O)_4PO_2(OH)_2.(H_2O)_6]^{+1}$

MM_2: $[Al_2(OH)_5(H_2O)_4PO_2(OH)_2.(H_2O)_6]^0$
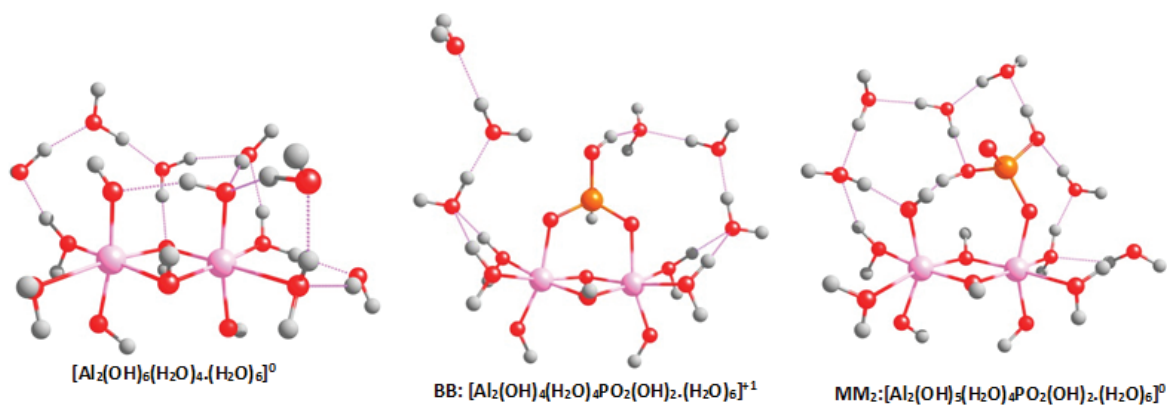
Fig. S2. DFT calculated structures of inner-sphere and H-bond adsorption products of phosphate on Al-hydr(oxide) under basic pH conditions.
Note: Red, pink, orange and gray denote O, Al, P, and H atoms, respectively.
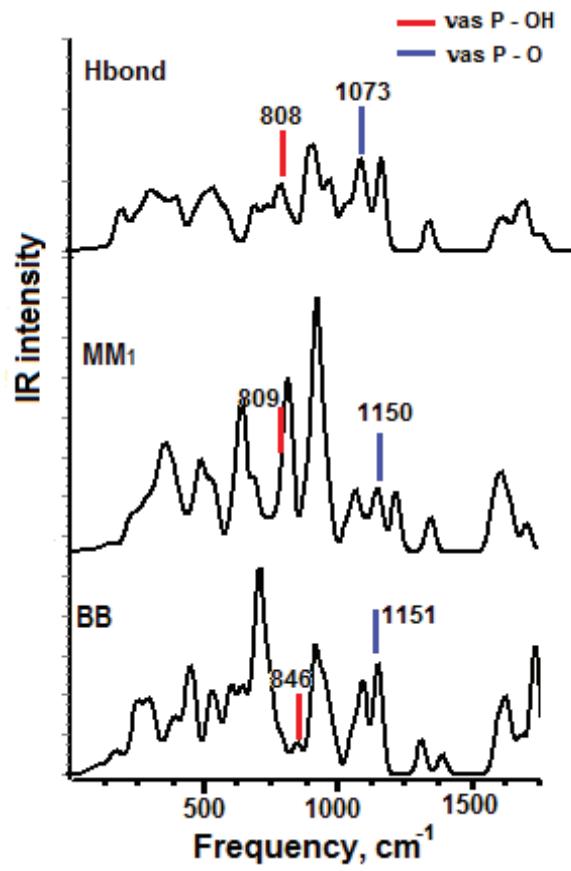
Fig. S3. IR spectra of complexes under acidic pH conditions.
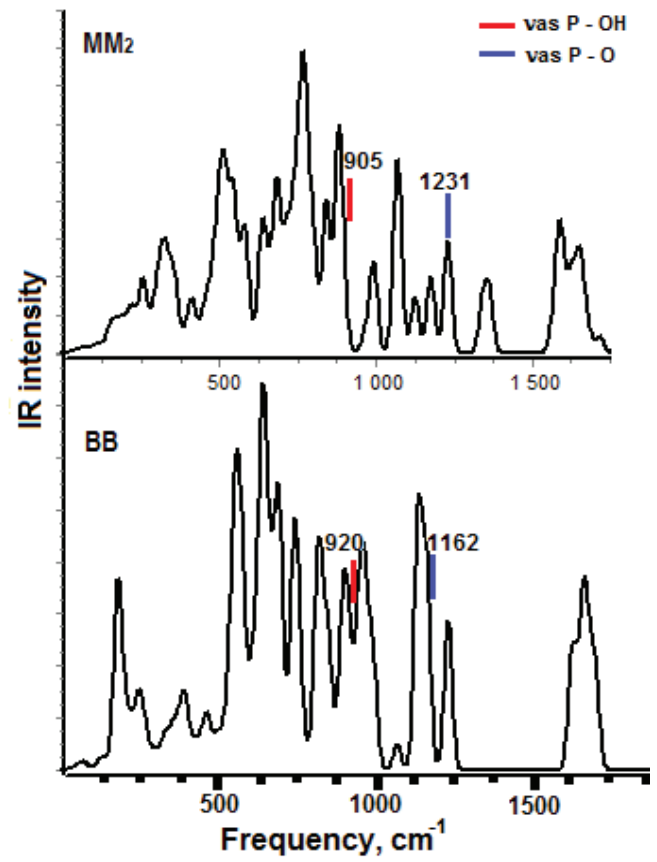
Fig. S4. IR spectra of complexes under basic pH conditions.

Cartesian coordinates for all clusters and Complexes
Level of theory: B3LYP/6-31+g(d,p)

CLUSTER
Acidic pH [Al$_2$(OH)$_4$(H$_2$O)$_6$.(H$_2$O)$_6$]+2

2 1

13	0	−1.219674	−0.956823	0.147479
8	0	−2.246456	−2.392334	1.188940
8	0	−2.709169	−0.266446	−0.562077
8	0	0.162073	0.091003	−0.613667
8	0	0.372370	−1.709751	0.840156
13	0	1.735430	−0.634887	0.099351
8	0	2.846460	0.654387	−0.844833
8	0	3.182473	−1.391985	0.831595
8	0	−1.218951	−2.292262	−1.326756
8	0	1.919865	−1.844254	−1.542427
1	0	−0.576436	−3.014768	−1.307512
1	0	1.769864	−1.448925	−2.415366
1	0	−0.009320	0.913805	−1.098345
1	0	0.441230	−2.488468	1.399945
1	0	−3.163727	0.452639	−0.106353
1	0	−3.015688	−2.712080	0.659799
1	0	−2.562334	−2.164408	2.075729
1	0	3.843274	0.516295	−0.692563
1	0	2.657025	1.602095	−0.675533
1	0	3.147220	−2.165546	1.402623
8	0	1.577345	0.736028	1.667485
8	0	−1.330607	0.150764	1.802647
1	0	−0.457765	0.423018	2.136838
1	0	−1.937208	0.937151	1.768181
1	0	1.665862	1.671765	1.353940
1	0	2.294186	0.569022	2.302039
1	0	2.780344	−2.293853	−1.559136
1	0	−2.118935	−2.646991	−1.536015
8	0	−0.261845	2.904272	−1.522013
1	0	−1.139010	3.281534	−1.297217
1	0	−0.089226	3.152931	−2.441921
1	0	−3.494661	3.925008	−1.311198
8	0	−2.766462	4.012338	−0.675915
1	0	−2.725926	4.956956	−0.458701
1	0	1.069084	3.205729	−0.385593
8	0	1.844676	3.010555	0.192964
1	0	2.304775	3.840830	0.382371
1	0	4.907136	−0.636607	0.450707
8	0	5.209237	0.146812	−0.053291
1	0	6.097344	−0.000949	−0.402643
1	0	−3.047905	2.839665	0.800234

(*Continued*)

(*Continued*)

8	0	−3.149410	2.067793	1.392405
1	0	−3.828807	2.289112	2.044689
1	0	−3.788072	−1.607512	−1.014436
8	0	−3.818512	−2.599940	−1.008102
1	0	−4.631837	−2.921063	−1.420234

Intermediate pH [Al$_2$(OH)$_5$(H$_2$O)$_5$.(H$_2$O)$_6$]$^{+1}$

1 1

13	0	1.519180	−0.081260	0.717075
8	0	2.532601	−1.808669	0.354449
8	0	3.188355	0.922286	0.304923
8	0	0.381184	1.474341	0.784877
8	0	−0.151572	−1.037371	0.938035
13	0	−1.368904	0.491128	0.801477
8	0	−2.378154	2.214557	0.563601
8	0	−3.086102	−0.483852	0.860756
8	0	2.171789	−0.165631	2.378580
8	0	−1.456713	0.521274	2.601081
1	0	1.643716	−0.028673	3.170734
1	0	−1.811212	1.245611	3.123683
1	0	0.441502	1.905680	1.649680
1	0	−0.222764	−1.276511	1.876506
1	0	3.610995	0.970563	1.180202
1	0	3.830161	0.526972	−0.344887
1	0	2.822855	−2.081471	1.241463
1	0	1.938806	−2.517384	−0.013906
1	0	−3.327222	2.129569	0.733039
1	0	−2.255477	2.680652	−0.310320
1	0	−3.225627	−0.721096	1.790665
1	0	−3.393204	−1.249333	0.266349
8	0	−1.265806	0.263030	−1.058133
8	0	1.185679	−0.090400	−1.198842
1	0	0.150463	0.069198	−1.299918
1	0	1.620600	0.615848	−1.701972
1	0	−1.614807	0.979704	−1.610667
8	0	−1.757402	−2.191481	−2.291559
1	0	−0.955829	−2.719906	−2.158094
1	0	−1.552154	−1.297184	−1.937910
8	0	4.600167	−0.337126	−1.534330
1	0	5.471391	−0.213794	−1.932981
1	0	4.442754	−1.288393	−1.455007
8	0	0.893458	2.953519	−1.443463
1	0	0.811993	2.562131	−0.538837
1	0	1.539766	3.669537	−1.399542
8	0	−1.754488	3.061004	−1.859162
1	0	−2.173474	3.673088	−2.477224
1	0	−0.775919	3.214411	−1.870273
8	0	−3.740872	−2.508454	−0.585260

(*Continued*)

(*Continued*)

1	0	−3.077083	−2.548789	−1.327704
1	0	−4.618839	−2.672948	−0.950636
8	0	0.460897	−3.300383	−0.476651
1	0	0.206182	−4.192320	−0.205204
1	0	−0.065352	−2.656582	0.050376

Basic pH $[Al_2(OH)_6(H_2O)_4 \cdot (H_2O)_6]^0$

0 1

13	0	1.381736	−0.416429	−0.323956
8	0	3.175892	−0.965760	0.723851
8	0	2.406327	0.944671	−1.397284
8	0	−0.298774	−0.009105	−1.161855
8	0	0.347631	−1.645255	0.741660
13	0	−1.375884	−1.159773	−0.006143
8	0	−3.074064	−0.687425	−0.919780
8	0	−2.434541	−2.613678	1.127624
8	0	1.114473	0.912127	1.002209
8	0	−1.519065	0.058851	1.326370
1	0	0.160652	0.829326	1.252408
1	0	−2.221306	0.720990	1.348924
1	0	−0.327966	−0.353146	−2.064909
1	0	0.342005	−1.366812	1.666161
1	0	2.213213	1.879683	−1.146859
1	0	3.386111	0.823166	−1.405117
1	0	3.132670	−0.770713	1.700752
1	0	3.114875	−1.918828	0.547366
1	0	−3.887273	−0.201844	−0.606509
1	0	−3.290198	−1.431881	−1.500139
1	0	−2.084397	−2.810074	2.005573
1	0	−2.141697	−3.301134	0.489905
8	0	−1.437991	−2.580416	−1.167460
8	0	1.914687	−1.746099	−1.423542
1	0	2.272473	−1.512640	−2.285213
1	0	−0.563826	−2.889729	−1.438028
1	0	−0.390843	3.111108	−0.838758
8	0	−1.216080	2.652925	−1.084944
1	0	−0.945579	1.709090	−1.162072
1	0	−2.436176	2.705876	0.028284
8	0	−3.183392	2.591646	0.688163
1	0	−3.231460	3.389483	1.226224
1	0	1.941265	3.849787	0.294896
8	0	1.443973	3.162633	−0.163842
1	0	1.314172	2.370194	0.466825
1	0	−5.659129	1.212480	−0.768862
8	0	−5.058142	0.857314	−0.103122

(*Continued*)

(*Continued*)

1	0	−4.497333	1.612089	0.208757
8	0	2.706073	0.257810	2.969394
1	0	2.304185	0.086214	3.828236
1	0	2.005834	0.643857	2.356390
1	0	4.663967	−0.232050	−0.240253
8	0	5.006224	0.369649	−0.930531
1	0	5.603824	−0.142960	−1.487982

COMPLEXES

Acidic pH
BB
1 1

13	0	−1.675906	−1.989473	−0.230209
8	0	−3.131792	−1.793349	1.221268
8	0	−2.808119	−2.765444	−1.351362
8	0	−0.033911	−2.057309	−1.154905
8	0	−0.386150	−1.544821	1.075519
13	0	1.154246	−1.150982	0.024669
8	0	2.517737	−1.082252	−1.355430
8	0	2.266875	−0.624046	1.340918
8	0	−1.532307	−3.905553	0.454298
8	0	1.980365	−3.018378	0.508647
1	0	−0.630700	−4.185375	0.673436
1	0	2.589027	−3.383092	−0.151584
1	0	0.043203	−2.197971	−2.101941
1	0	−0.512856	−1.321712	2.001185
1	0	−3.281355	−2.298432	−2.044148
1	0	−3.641730	−0.990117	1.030523
1	0	−3.749330	−2.538999	1.155285
1	0	3.473608	−0.792052	−0.934808
1	0	2.341576	−0.533417	−2.130734
1	0	2.010954	0.142084	1.876768
8	0	0.451549	0.594092	−0.502727
8	0	−2.034044	−0.133235	−0.594573
1	0	2.513371	−2.745502	1.279148
1	0	−1.871737	−4.444378	−0.281617
15	0	−1.022869	1.012144	−0.416259
8	0	−1.205470	1.816417	0.938930
8	0	−1.355260	2.124334	−1.550548
1	0	−1.789577	1.736679	−2.326085
1	0	−2.074072	2.352369	1.054578
8	0	−3.336554	3.195350	1.105893
1	0	−3.662895	3.604352	1.917019
1	0	−3.265662	3.893516	0.409203
1	0	−1.983193	4.202255	−1.396961
8	0	−2.734189	4.697049	−1.035122

(*Continued*)

(*Continued*)

1	0	−2.583436	5.633956	−1.212652
1	0	0.332094	2.003847	2.171856
8	0	1.247740	1.934447	2.497822
1	0	1.263571	2.286640	3.396977
1	0	2.247018	2.743666	0.955095
8	0	2.407987	2.814447	−0.002596
1	0	1.822368	2.134824	−0.375725
1	0	4.070648	2.521533	−0.540992
8	0	4.895479	2.082220	−0.855142
1	0	5.611565	2.727603	−0.847688
1	0	4.866390	0.452222	−0.342912
8	0	4.540511	−0.457442	−0.117079
1	0	3.982207	−0.372949	0.692182

MM1

1 1

13	0	0.393246	−1.752050	0.399328
8	0	−0.581154	−1.903514	2.160086
8	0	−0.324896	−3.259637	−0.166772
8	0	1.654242	−1.291014	−0.977043
8	0	1.494614	−0.416898	1.203836
13	0	2.555239	0.169305	−0.225661
8	0	3.593454	0.426283	−1.912434
8	0	3.595775	1.372242	0.643439
8	0	1.725253	−3.131801	1.206804
8	0	4.100174	−1.170551	0.263676
1	0	2.655683	−2.983220	0.984020
1	0	4.608537	−1.484371	−0.500329
1	0	1.464789	−1.522715	−1.891312
1	0	1.708329	−0.385157	2.140278
1	0	−0.994299	−3.294436	−0.871281
1	0	−1.030551	−2.764009	2.117792
1	0	−1.267442	−1.208321	2.280747
1	0	4.275990	1.178274	−1.832000
1	0	3.053971	0.612843	−2.694129
1	0	3.131847	1.981843	1.232065
8	0	1.193631	1.391662	−0.878951
8	0	−0.822080	−0.407295	−0.241307
1	0	1.106619	2.221071	−0.327079
1	0	0.325729	0.925415	−0.841031
1	0	4.696576	−0.635938	0.816734
1	0	1.391302	−3.899001	0.700479
15	0	−2.192943	0.209957	0.116110
8	0	−3.300935	−0.820327	−0.341838
8	0	−2.390356	1.633996	−0.365645
8	0	−2.291520	0.190062	1.762348
1	0	−2.083249	1.074501	2.131012
1	0	−4.272096	−0.479018	−0.365917
8	0	−2.331448	−2.903832	−2.145123
1	0	−2.861689	−2.249599	−1.659307

(*Continued*)

(*Continued*)

1	0	−2.948181	−3.547660	−2.514183
8	0	−5.662153	0.073910	−0.588256
1	0	−6.359652	0.014456	0.075933
1	0	−5.575259	1.020031	−0.875373
1	0	−3.906414	2.335227	−1.104632
8	0	−4.855937	2.521863	−1.266192
1	0	−4.936730	2.914145	−2.144187
1	0	−1.994300	2.770110	0.895792
8	0	−1.585798	3.009990	1.766971
1	0	−2.130938	3.695617	2.175757
1	0	1.195065	4.306607	0.636041
8	0	1.013288	3.385376	0.863743
1	0	0.128772	3.365994	1.298587
1	0	4.720420	2.236382	−0.356897
8	0	5.079597	2.385262	−1.271026
1	0	6.031026	2.541046	−1.237417

H-bond

1 1

13	0	2.337856	−0.490934	−0.453342
8	0	2.005965	−2.232662	0.363068
8	0	3.702240	−0.979872	−1.529980
8	0	2.056044	1.342371	−1.126489
8	0	1.075406	0.291827	0.715581
13	0	0.878168	2.047246	0.133364
8	0	0.678924	3.649672	−1.049916
8	0	1.490190	2.948522	1.513280
8	0	3.738529	−0.085915	0.829483
8	0	3.520640	1.679198	2.662521
1	0	3.670504	0.561254	1.612118
1	0	3.446466	1.489755	3.605588
1	0	2.807262	1.790338	−1.530737
1	0	0.535753	−0.168138	1.374279
1	0	3.517886	−1.069000	−2.471291
1	0	1.110111	−2.616821	0.224893
1	0	2.717967	−2.902554	0.131202
1	0	−0.183004	4.181295	−1.110771
1	0	1.002491	3.545822	−1.954766
1	0	1.571938	3.906738	1.461157
8	0	−1.987104	−0.424963	−0.378570
8	0	−0.621726	−2.630084	−0.374455
1	0	2.734973	2.223355	2.383154
1	0	4.621724	−0.065054	0.436584
15	0	−1.678009	−1.747463	0.306533
8	0	−1.155167	−1.327446	1.801806
8	0	−3.018884	−2.590461	0.561297
1	0	−2.931561	−3.534329	0.233254
1	0	−1.161117	−2.055811	2.441161
8	0	−0.958721	1.815936	0.053179
8	0	0.937795	−1.050616	−1.804642
1	0	−1.349698	0.866684	−0.061902

(*Continued*)

1	0	−1.720804	2.451296	0.145171
1	0	0.482096	−0.355929	−2.297791
1	0	0.246210	−1.677372	−1.441917
8	0	4.009460	−3.513406	−0.647239
1	0	4.820090	−3.881211	−0.275649
1	0	4.212984	−2.649785	−1.084199
1	0	−1.466947	−4.600278	−0.726976
8	0	−2.293055	−4.942845	−0.345072
1	0	−2.679320	−5.571030	−0.968228
1	0	−4.809031	−1.588467	0.820678
8	0	−5.470940	−0.876947	0.853255
1	0	−6.335579	−1.297507	0.934292
1	0	−4.989196	0.561927	−0.248837
8	0	−4.353305	1.065109	−0.799373
1	0	−3.598269	0.448538	−0.869008
1	0	−3.779485	2.434857	−0.271401
8	0	−3.213841	3.213556	0.068241
1	0	−3.609984	3.510633	0.898489
1	0	−2.352689	4.427438	−0.909211
8	0	−1.569922	4.873489	−1.306929
1	0	−1.750184	5.817524	−1.389981

Intermediate pH
BB
1 1

13	0	−0.340447	−1.874033	−0.169943
8	0	−1.871786	−2.016308	1.129910
8	0	−1.623047	−1.901516	−1.705038
8	0	1.191774	−1.553264	−1.234142
8	0	0.997589	−1.562895	1.209774
13	0	2.434541	−0.944126	0.047644
8	0	3.626946	−0.119624	−1.276500
8	0	3.633642	−0.280179	1.586090
8	0	−0.424837	−3.664333	−0.129446
8	0	3.578901	−2.310712	0.227333
1	0	0.305702	−4.218339	−0.417521
1	0	3.471920	−3.133121	−0.257825
1	0	1.149672	−1.208722	−2.131788
1	0	1.217575	−2.380346	1.676320
1	0	−1.751502	−2.850979	−1.867478
1	0	−2.506915	−1.508909	−1.476708
1	0	−2.011592	−2.974725	1.216154
1	0	−2.699050	−1.597254	0.779589
1	0	4.481335	−0.575040	−1.261261
1	0	3.755761	0.865345	−1.356878
1	0	4.108185	−1.092353	1.840377
1	0	3.277160	0.162428	2.366982
8	0	1.660955	0.824798	0.192080
8	0	−0.769319	0.019169	−0.093161
15	0	0.183050	1.013555	0.568051
8	0	−0.258795	2.512910	0.213994

8	0	−0.022232	1.004868	2.165453
1	0	0.475891	3.098094	−0.087066
1	0	0.007897	0.083071	2.480951
8	0	3.926129	2.507031	−1.523788
1	0	4.338369	2.909149	−2.298677
1	0	3.157461	3.053483	−1.282842
8	0	1.720022	4.262890	−0.617841
1	0	2.092498	4.773583	0.117048
1	0	1.371667	4.914503	−1.244806
1	0	−1.991902	3.187880	0.726868
8	0	−2.921120	3.467724	0.807022
1	0	−3.061644	3.736125	1.723536
1	0	−4.022731	2.391963	0.001552
8	0	−4.535133	1.737954	−0.533081
1	0	−4.635197	2.133535	−1.408999
1	0	−3.795535	0.076522	−0.471107
8	0	−3.769717	−0.909043	−0.443609
1	0	−4.725228	−1.132642	−0.458233
1	0	−6.235160	0.513642	−0.235683
8	0	−6.442814	−0.418203	−0.417421
1	0	−7.320870	−0.604288	−0.064425

MM1
0 1

13	0	1.267786	−1.799997	0.018992
8	0	2.932304	−1.909752	−1.105023
8	0	2.275874	−2.168960	1.761190
8	0	−0.327846	−1.507943	1.027133
8	0	−0.022838	−1.413878	−1.322943
13	0	−1.460253	−0.740720	−0.201196
8	0	−2.741445	−0.316414	1.246697
8	0	−4.879823	−1.944562	0.383867
8	0	1.333393	−3.607399	−0.062950
8	0	−2.744200	−1.664901	−1.039776
1	0	0.505841	−4.080586	−0.186768
1	0	−2.437362	−2.186931	−1.788850
1	0	−0.369850	−1.341963	1.972993
1	0	0.242249	−0.890561	−2.089475
1	0	2.363935	−3.131113	1.621398
1	0	3.144315	−1.752433	1.937787
1	0	2.964484	−2.694970	−1.666705
1	0	3.277119	−1.067575	−1.541791
1	0	−3.451969	−0.984292	1.322868
1	0	−3.234102	0.578220	1.193903
1	0	−4.147674	−1.951261	−0.310120
1	0	−5.159412	−2.856155	0.527651
8	0	−1.195549	1.004992	−0.583616
8	0	1.847827	0.038708	0.203923
1	0	−0.941359	1.589277	0.167393
15	0	2.224401	1.047257	−0.956007
8	0	2.375333	2.494869	−0.260464

(*Continued*)

8	0	3.448214	0.569568	−1.703670
8	0	0.974236	1.244857	−1.913832
1	0	0.073656	1.207701	−1.419654
1	0	3.097618	2.568448	0.421523
1	0	3.369734	−0.052811	1.078041
8	0	4.186959	−0.200507	1.620142
1	0	4.885964	−0.380108	0.974796
1	0	4.332138	1.647865	1.975334
8	0	4.196945	2.587065	1.731474
1	0	3.928243	3.056061	2.531056
1	0	0.647321	3.144815	0.524554
8	0	−0.240606	3.105989	0.925045
1	0	−0.778702	3.781289	0.486895
1	0	−3.856390	2.440799	0.375110
8	0	−4.178500	1.824831	1.065645
1	0	−5.047303	1.477238	0.765296
1	0	−2.284189	2.345534	−1.112895
8	0	−2.800064	3.173927	−0.974030
1	0	−3.155681	3.442358	−1.829451
1	0	−6.006865	−0.517274	0.247099
8	0	−6.390283	0.386777	0.228822
1	0	−7.225129	0.350742	0.709701

MM2
1 1

13	0	2.131032	−1.209630	−0.287692
8	0	3.280506	0.138834	−1.233428
8	0	3.495385	−1.304508	1.177463
8	0	0.829661	−2.185211	0.636807
8	0	0.624587	−0.913520	−1.397797
13	0	−0.732224	−1.872132	−0.402014
8	0	−1.877389	−2.727614	0.936187
8	0	−2.263843	−1.329818	−1.568003
8	0	3.139881	−2.369651	−1.186585
8	0	−0.848670	−3.339097	−1.428648
1	0	2.876489	−3.279589	−1.345610
1	0	−0.208560	−4.053227	−1.374767
1	0	0.863454	−2.586398	1.509667
1	0	0.733965	−1.285034	−2.282406
1	0	4.235302	−1.810587	0.805240
1	0	3.816959	−0.489351	1.628473
1	0	3.705264	−0.335392	−1.965736
1	0	2.906316	1.004253	−1.521699
1	0	−2.305092	−3.502909	0.545620
1	0	−2.478450	−2.272099	1.596482
1	0	−2.273261	−1.922052	−2.335802
1	0	−2.402110	−0.379652	−1.793623
8	0	−1.086731	−0.175528	0.561572
8	0	1.507739	0.448949	0.731851
1	0	0.544700	0.324863	0.930836
1	0	2.009286	0.733621	1.530785

(*Continued*)

15	0	−1.923544	1.090448	0.255725
8	0	−3.183368	1.032822	1.252726
8	0	−2.370807	1.301960	−1.188280
8	0	−1.020774	2.328208	0.754935
1	0	−3.993545	1.450198	0.843183
1	0	−0.917931	3.011457	0.058813
1	0	−4.595496	1.974412	−1.099788
8	0	−5.119559	1.937832	−0.283921
1	0	−5.740534	2.677043	−0.287077
1	0	−4.112691	−1.637190	3.133749
8	0	−3.301159	−1.394040	2.672124
1	0	−3.400914	−0.482845	2.334081
1	0	−1.294511	2.672136	−1.971848
8	0	−0.644258	3.390896	−1.808275
1	0	−0.935642	4.169041	−2.301215
1	0	1.271299	2.931354	−1.600525
8	0	1.999300	2.505593	−1.108230
1	0	1.553355	1.972980	−0.420137
1	0	3.833117	1.972197	1.805960
8	0	3.570360	1.155136	2.313103
1	0	3.672074	1.349419	3.254146
1	0	3.334300	3.270431	0.001582
8	0	3.925816	3.302865	0.780808
1	0	4.718104	3.796232	0.536659

H-bond
0 1

13	0	−0.307408	2.183770	−0.315173
8	0	1.374250	2.479210	0.622123
8	0	−0.163218	3.709355	−1.313933
8	0	−2.005363	1.597326	−1.044863
8	0	−0.710592	0.668668	0.718739
13	0	−2.093056	−0.099023	−0.354336
8	0	−3.649410	−0.609842	−1.504165
8	0	−3.120607	−0.481711	1.087004
8	0	−1.260501	3.335966	1.001214
8	0	−3.405451	2.110200	2.065260
1	0	−2.049088	2.908752	1.439479
1	0	−4.302905	2.461708	2.092977
1	0	−2.482070	1.955110	−1.797177
1	0	0.005257	0.066604	1.009486
1	0	−0.041434	3.566719	−2.259109
1	0	2.065078	1.773492	0.498300
1	0	1.771409	3.375937	0.462261
1	0	−4.183659	−1.350571	−1.044919
1	0	−3.224130	−1.017692	−2.275225
1	0	−2.578808	−0.638635	1.872050
8	0	1.271236	−1.291627	1.202863
8	0	2.867181	0.390305	−0.018855
1	0	−3.461714	1.189838	1.709646
1	0	−1.574468	4.102543	0.499733

(*Continued*)   (*Continued*)

(*Continued*)

15	0	2.674802	−0.871879	0.854253
8	0	3.487348	−0.674441	2.246646
8	0	3.443034	−2.091178	0.082124
1	0	4.140741	−1.738793	−0.525832
1	0	4.357611	−0.270697	2.117594
8	0	−1.040198	−1.054628	−1.443509
8	0	0.640617	0.981775	−1.620985
1	0	−0.678693	−1.913363	−1.156534
1	0	0.099372	0.127541	−1.694279
1	0	1.515346	0.710318	−1.260611
8	0	1.969092	4.898287	−0.286781
1	0	1.835774	5.732845	0.177312
1	0	1.132218	4.681727	−0.784732
1	0	4.401164	0.166257	−1.118172
8	0	5.095615	−0.484449	−1.354638
1	0	5.243059	−0.428062	−2.306187
1	0	2.780900	−3.768131	−0.372311
8	0	2.272854	−4.555026	−0.653871
1	0	2.632669	−5.303923	−0.163893
1	0	0.571318	−3.937223	−0.321357
8	0	−0.148157	−3.351628	−0.001996
1	0	0.313109	−2.705343	0.579230
1	0	−1.789097	−4.021569	0.125322
8	0	−2.719169	−4.348279	0.108667
1	0	−2.747122	−5.136893	0.661951
1	0	−4.120928	−3.202037	−0.013461
8	0	−4.720247	−2.421295	−0.013255
1	0	−4.373429	−1.865894	0.715955

Basic pH
BB
1 1

13	0	−1.991545	−1.135277	−0.309863
8	0	−2.966179	−0.440900	−1.931455
8	0	−3.356687	−0.247619	0.895363
8	0	−0.816019	−1.609182	1.151981
8	0	−0.565386	−1.913156	−1.271784
13	0	0.732353	−2.114921	0.097297
8	0	2.031185	−2.116017	1.641147
8	0	2.262897	−2.311939	−1.188048
8	0	−1.175943	0.621818	−0.341072
8	0	1.212383	−0.242110	0.039487
1	0	−1.146342	−2.310930	1.727499
1	0	−0.322455	−1.623560	−2.157615
1	0	−3.779958	0.548139	0.494821
1	0	−4.024510	−0.951248	0.979186
1	0	−3.670720	−1.098263	−2.059859
1	0	−3.384619	0.439769	−1.800184
1	0	2.892158	−1.689341	1.423634
1	0	2.173873	−3.056345	1.840832
1	0	3.085187	−1.849959	−0.884789

(*Continued*)

(*Continued*)

1	0	2.431505	−3.268293	−1.201024
8	0	0.778693	−3.885432	0.351844
8	0	−3.194150	−2.467546	−0.258693
1	0	−2.959167	−3.372681	−0.480872
1	0	0.104292	−4.473807	0.002116
15	0	0.194038	0.861463	0.299934
8	0	−0.017090	1.141767	1.889413
8	0	0.866994	2.230187	−0.174269
1	0	0.447883	3.023599	0.229736
1	0	−0.413716	0.347216	2.294903
1	0	−0.614815	3.170732	2.094424
8	0	−0.614611	3.911314	1.460442
1	0	−0.321089	4.696352	1.943723
1	0	−2.188696	4.066938	0.388005
8	0	−2.966869	4.061612	−0.201175
1	0	−2.838698	4.761849	−0.852946
1	0	5.954782	3.083185	−2.433440
8	0	5.662369	3.186814	−1.519051
1	0	6.298696	3.772325	−1.089000
1	0	−3.718897	2.604625	−0.602352
8	0	−4.216027	1.757971	−0.762956
1	0	−5.142618	2.007730	−0.879546
1	0	4.504553	2.129476	−0.603816
8	0	3.899913	1.571825	−0.074462
1	0	2.994042	1.870144	−0.246563
1	0	4.080298	−0.035507	0.122023
8	0	4.163580	−1.029407	0.251820
1	0	5.105505	−1.221511	0.347175

MM2
0 1

13	0	−0.565445	−2.349220	−0.077352
8	0	−2.156116	−2.467368	−1.412716
8	0	−1.202287	−3.820613	1.382635
8	0	0.943842	−2.005059	0.994458
8	0	0.442617	−1.210431	−1.215084
13	0	1.945807	−0.821282	−0.090766
8	0	3.422080	−0.580277	1.308167
8	0	2.940160	0.438567	−1.422875
8	0	−1.751351	−1.174294	0.734379
8	0	1.307021	0.806459	0.523922
1	0	−1.449465	−0.719865	1.542068
1	0	1.066794	−2.186721	1.929213
1	0	−0.021917	−0.445048	−1.578845
1	0	−2.129995	−3.945842	1.615835
1	0	−0.901235	−4.551853	0.801118
1	0	−3.078719	−2.236386	−1.172463
1	0	−2.087550	−3.333884	−1.839085
1	0	3.862704	0.292246	1.319110
1	0	4.028614	−1.218142	0.883271
1	0	2.632647	1.391117	−1.527531

(*Continued*)

(*Continued*)

(*Continued*)

1	0	3.084790	−0.012204	−2.266163
8	0	3.158786	−1.999370	−0.771912
8	0	−0.184567	−3.972854	−0.833297
1	0	0.588011	−4.030280	−1.403286
1	0	2.898685	−2.925328	−0.768168
15	0	−0.034949	1.513807	0.825903
8	0	−0.712660	1.199115	2.120863
8	0	−1.055683	1.165039	−0.432039
8	0	0.314141	3.057688	0.528189
1	0	−0.465390	3.696367	0.565777
1	0	−1.540335	0.346374	−0.146822
1	0	1.703650	3.153576	−0.703931
8	0	2.499935	3.027028	−1.264632
1	0	3.246479	3.185901	−0.666184

(*Continued*)

(*Continued*)

1	0	4.566544	1.135359	−0.541628
8	0	4.863836	1.631955	0.243425
1	0	5.824838	1.706791	0.194373
1	0	−1.630650	5.547870	0.047695
8	0	−1.767274	4.663814	0.408320
1	0	−2.378024	4.182439	−0.215199
1	0	−2.347204	2.377484	−1.191972
8	0	−3.053099	3.045126	−1.276900
1	0	−3.866520	2.569317	−1.007321
1	0	−3.306849	−1.201074	0.474817
8	0	−4.205633	−1.285258	0.007531
1	0	−4.808192	−1.758285	0.594544
1	0	−5.352953	1.662673	0.596910
8	0	−5.142479	1.400679	−0.307944
1	0	−4.849392	0.467269	−0.255064